Evidence for non-cold dark matter from DESI DR2 measurements

Utkarsh Kumar,[1,*] Abhijith Ajith,[2,†] and Amresh Verma[3,‡]

[1] *Department of Physics, University of Ottawa, Ottawa, ON K1N6N5, Canada;*
[2] *Indian Institute of Science Education and Research Bhopal, Bhopal 462066, India*
[3] *Physics Department, Ariel University, Ariel 40700, Israel*

(Dated: Tuesday 22nd April, 2025)

We investigate potential deviations from cold dark matter (CDM) using the latest Baryon Acoustic Oscillations (BAO) measurements from the Dark Energy Spectroscopic Instrument (DESI). Analyzing DESI data alone constrains the dark matter equation of state parameter $w_{\rm dm} = -0.042^{+0.047}_{-0.024}$, revealing a mild preference for non-cold dark matter. This preference strengthens significantly in combined analyses, but reveals a striking tension in the inferred $w_{\rm dm}$ values from observations of different nature. The DESI+DESY5 combination yields $w_{\rm dm} = -0.084 \pm 0.035$, excluding CDM ($w_{\rm dm} = 0$) at 2.4σ significance. In contrast, Planck+DESI gives $w_{\rm dm} = 0.00077 \pm 0.00038$, differing from concordance model at 2σ significance. The non-vanishing $w_{\rm dm}$ preference is particularly driven by low-redshift BAO measurements ($z < 1.1$), while higher redshift data remain consistent with ΛCDM. The evidence for non-cold dark matter is more pronounced in DESI compared to the previous BAO surveys. All dataset combinations show significant improvement over the ΛCDM paradigm, providing compelling evidence for non-cold dark matter scenario.

Introduction– The standard model of cosmology explains the numerous phenomena of the observed Universe while providing an excellent fit to the various astrophysical and cosmological observations. The measurements from the cosmic microwave background (CMB) [1–9], baryon acoustic oscillations (BAO) [10–17], Type Ia supernovae [18–24] and weak lensing [25–32], have significantly improved our understanding of the Universe. The standard model of cosmology suggests that most of the universe comprises two unknown components, called dark matter (DM) and dark energy (DE), which are responsible for structure formation and the current accelerated expansion of the Universe, respectively. Several cosmological observations such as Supernovae type Ia measurements and the more recent BAO measurements from the second data release (DR2) of the Dark Energy Spectroscopic Instrument (DESI) have shown strong evidence towards the existence of the Universe's accelerated expansion. On the other hand, in the absence of any direct observations of dark matter, we are only left to presume about its property based on its weak interactions with standard model particles and gravitational effects. In the standard cosmological scenario, due to its weak interaction with other known particles, the dark matter component is parameterised as a pressure-less fluid with vanishing equation of state (EoS), referred to as cold dark matter(CDM).

CDM explains the formation of structures consistently at scales much higher than 1 Mpc. Nevertheless, it encounters issues while looking at observations on smaller scales [33–35] like the core-cusp [36], missing satellite [37, 38] and the too-big-to-fail problems [39]. Such discrepancies have prompted the consideration of alternative dark matter models. Warm dark matter(WDM) composed of particles with non-negligible thermal velocities offers a viable resolution to these problems. Unlike CDM, WDM suppresses structure formation below its free streaming scale. Hence, WDM models erase the substructure at smaller scales, delay the structure formation, and resolve the small-scale problems that plague the standard cosmology. Sterile neutrinos are said to be one of the viable candidates of warm dark matter [40, 41].

The strong preference for evolving dark energy from DESI [17, 42], has prompted the surge in the exploration of a plethora of models of DE [43–63], and DE-DM interactions [64–71]. In this letter, we use the DESI measurements to probe the nature of dark matter. In the absence of any underlying theory of dark matter, we investigate a phenomenological model with a dark matter component of an arbitrary EoS in the light of recent data release of DESI measurements. We demonstrate that the DESI data give a robust preference for the non-vanishing pressure of dark matter candidate.

Cosmology with non-cold dark matter– We consider the Universe to be filled with a dark matter component of energy density $\rho_{\rm dm}$ and EoS parameter $w_{\rm dm}$ [72–75]. The evolution of the energy density of such a dark matter component, determined by solving the continuity equation, scales as

$$\rho_{\rm dm} = \rho_{\rm dm,0}\, a^{-3(1+w_{\rm dm})} \tag{1}$$

with $\rho_{\rm dm,0}$ being the current energy density and a being the scale factor. In the presence of $\rho_{\rm dm}$, the Friedmann equations take the following form:

$$\mathcal{H}^2 = \frac{8\pi G a^2}{3}\left(\rho_{\rm r} + \rho_{\rm b} + \rho_{\rm dm} + \rho_\Lambda\right) \tag{2}$$

$$\dot{\mathcal{H}} - \mathcal{H}^2 = -4\pi G a^2\left(\frac{4}{3}\rho_{\rm r} + \rho_b + (1+w_{\rm dm})\,\rho_{\rm dm}\right) \tag{3}$$

Here $\rho_{\rm r,b}$ are the energy densities of radiation and baryonic components of the universe which scale as $\rho_{\rm r,0}\, a^{-4}$

* utkarshkumar.physics@gmail.com
† abhijith.ajith.421997@gmail.com
‡ amreshverma702@gmail.com

and $\rho_{\rm b,0}\, a^{-3}$ respectively. Note that the derivatives considered here are with respect to conformal time and $\mathcal{H}$ is the corresponding Hubble parameter. Due to the non-vanishing pressure of dark matter, the perturbation equations also get modified, and are expressed as follows in the synchronous gauge without the inclusion of shear perturbations [76, 77]:

$$\dot{\delta}_{\rm dm} = -\left(1+w_{\rm dm}\right)\left(\theta_{\rm dm}+\dot{h}/2\right) - 3\,\mathcal{H}\left(c_{\rm s}^2-c_{\rm a}^2\right) \left[\delta_{\rm dm}+3\,\mathcal{H}\left(1+w_{\rm dm}\right)\frac{\theta_{\rm dm}}{k^2}\right] \tag{4}$$

$$\dot{\theta}_{\rm dm} = -\mathcal{H}\left(1-3c_{\rm s}^2\right)\theta_{\rm dm} + \frac{k^2 c_{\rm s}^2}{1+w_{\rm dm}}\,\delta_{\rm dm} \tag{5}$$

Here $\delta_{\rm dm}$ and $\theta_{\rm dm}$ represent the density contrast and velocity divergence of dark matter, respectively. We model dark matter to be a perfect fluid with a constant equation of state, in which the definition of adiabatic speed of sound becomes $c_{\rm a}^2 = w_{\rm dm}$. Further, we assume the effective speed of sound $c_{\rm s}^2$ to be 0.

Methodology and data– We implement the theoretical model in a modified version of the Boltzmann solver code `CAMB` [78, 79]. We perform Markov-Chain-Monte Carlo (MCMC) simulations using the publicly available tool `COBAYA` [80, 81]. Our model has 7 free cosmological parameters. We constrain the cosmological parameters with uniform priors: the baryonic matter density $\Omega_b h^2 \in [0.005, 0.1]$, the dark matter density $\Omega_{\rm dm} h^2 \in [0.001, 0.99]$, the logarithmic amplitude of primordial curvature spectrum $\ln(10^{10} A_s) \in [1.6, 3.9]$ evaluated at a suitable pivot scale, $k = 0.05$ Mpc^{-1} along with its tilt $n_s \in [0.8, 1.2]$, the reionization optical depth $\tau_{\rm reio} \in [0.01, 0.8]$, the present value of the Hubble parameter $H_0 \in [20, 100]$ and EoS for dark matter $w_{\rm dm} \in [-0.5, 0.5]$. We use the standard three-neutrino description with a massive neutrino of mass $m_\nu = 0.06$ eV, while the other two being massless. The chains converge by ensuring the Gelman-Rubin criterion $|R-1| \leq 0.01$ or the effective sample size becoming greater than 10^5. We utilize `GetDist` [82] and `BOBYQA` [83, 84] to analyze chains and find the maximum likelihood posterior $\chi^2_{\rm MAP}$, respectively. We calculate the differences in $\chi^2_{\rm MAP}$ and deviance information criterion (DIC) to get the preference of our model over ΛCDM. The DIC is calculated as

$$\mathrm{DIC} = 2\overline{\chi^2(\theta)} - \chi^2(\hat{\theta}) \tag{6}$$

with $\overline{\chi^2(\theta)}$ and $\chi^2(\hat{\theta})$ being the average of the effective χ^2 over the posterior distribution and the best-fit χ^2 respectively. In addition, we also estimate the concordance/discordance between two datasets, D_1 and D_2 in a given model using the DIC-based statistic $\mathcal{I}(D_1, D_2)$ [85]. To be precise, a positive value of $\log_{10}\mathcal{I}$ indicates the consistency between the two datasets and conversely for a negative value. We further qualify the level of concordance or discordance using Jeffrey's scale, such that the value of $\log_{10}\mathcal{I}$ in excess of $\pm 1/2$ is considered to be 'substantial', excess of ± 1 is 'strong', and a value in excess of ± 2 shall be 'decisive' [86]. We use the following datasets in our analysis:

- **DESI:-** The 13 DESI-BAO DR2 ([87, 88]) measurements across the redshifts range $0.1 < z < 4.2$ obtained from observations of about 14 million galaxies and quasars which include bright galaxy sample (BGS), luminous red galaxies (LRG), emission line galaxies (ELG), quasars (QSO), and Lyman-α tracers. These measurements are given in terms of the volume averaged distance $D_{\rm V}(z)/r_{\rm d}$, angular diameter distance $D_{\rm M}(z)/r_{\rm d}$ and comoving Hubble distance $D_{\rm H}(z)/r_{\rm d}$, where $r_{\rm d}$ is the sound horizon at the drag era.

- **CMB:-** CMB temperature−temperature, temperature -polarization, and polarization-polarization spectra [1], along with the CMB lensing likelihood derived from the 4-point correlation function of the CMB [3]. We refer to these as P18 and PL18, respectively.

- **SNIa:-** We use the PantheonPlus(PP) dataset [19], which contains 1701 light curves for 1550 spectroscopically confirmed Type Ia supernovae (SNeIa) covering the redshift range $0.001 < z < 2.26$. Additionally, we incorporate the Union3 compilation comprising 2087 SNe [20] and the DES-Y5(DESY5) sample containing 1635 DES SNe spanning $0.10 < z < 1.13$ [23].

- **DESY3 3×2pt:-** We use galaxy-galaxy, galaxy-shear, and shear-shear two-point correlation function measurements obtained from DES Year 3 analysis. These observations were measured from over 10 million lens galaxies in the `MagLim` sample, that covers approximately 4000 deg^2 of sky [31, 32]. We use the CosmoLike [89] pipeline in our analysis of DESY3.

The 68% constraints on the cosmological parameters for various datasets considered in this letter are shown in Table I. We also perform statistical comparison of the ΛwDM scenario with the concordance model, where the terminology wDM corresponding to non-cold dark matter. Table II presents the best-fit $\Delta\chi^2_{\rm MAP} = \chi^2_{\Lambda{\rm wDM}} - \chi^2_{\Lambda{\rm CDM}}$ along with their significance $N\sigma$, and ΔDIC. From the DESI alone, we obtain the 68% CL constraints $w_{\rm dm} = -0.042^{+0.047}_{-0.024}$ and $\Omega_{\rm m} = 0.334^{+0.023}_{-0.040}$ by marginalizing over other cosmological parameters. The former excludes the canonical value of $w_{\rm dm} = 0$ at a statistical significance of $\approx 1.1\sigma$. The DESI data alone prefer the concordance model over the wDM scenario as we find $\Delta\mathrm{DIC} > 0$ despite a better fit yielding $\Delta\chi^2_{\rm MAP} = -0.577$. Next, we jointly analyze DESI and SNIa data. SNIa data alone cannot determine the EoS for dark matter. Interestingly, the joint analysis of DESI+ SNIa tightly constrains the $w_{\rm dm}$ as suggested in Table I. However the constraints on $w_{\rm dm}$ depend on the choice of SNIa dataset. In particular, the joint analysis of DESI and DESY5 yields

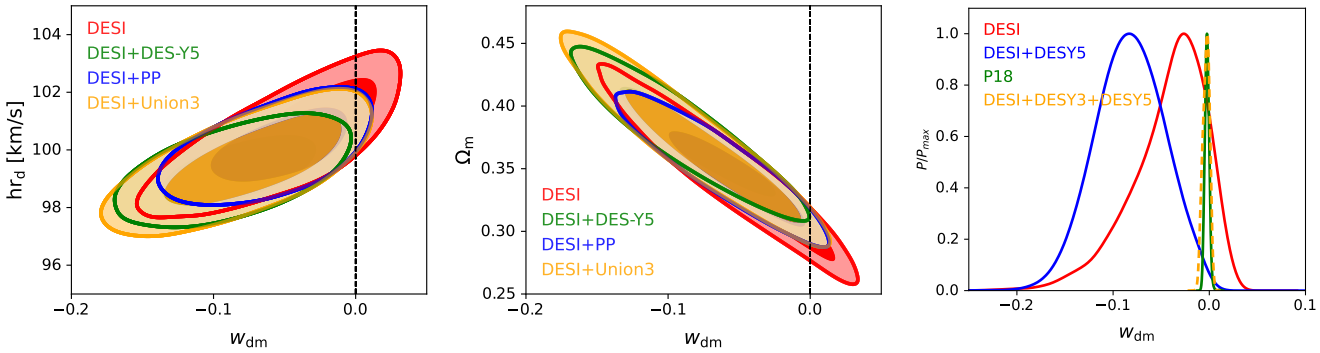

FIG. 1. Two-dimensional confidence contours (68% and 95% CL) for the cosmological parameter pairs $h\,r_{\rm d}$–$w_{\rm dm}$ (left panel) and $\Omega_{\rm m}$–$w_{\rm dm}$ (middle panel), derived from DESI and supernovae (SN) datasets. The vertical black dashed line indicates the cold dark matter equation of state ($w_{\rm dm} = 0$). Marginalized constraints on $w_{\rm dm}$ are shown for CMB (P18), DESI BAO, SNIa (DES-Y5), and LSS (DES-Y3). Color coding for each dataset corresponds to the legend.

Dataset	$\boldsymbol{H_0}$	$\boldsymbol{w_{\rm dm}}$ $(\#\,\sigma)$	$\boldsymbol{\Omega_m}$	$\boldsymbol{h\,r_{\rm d}}$	$\boldsymbol{S_8}$
DESI	80^{+20}_{-7}	$-0.042^{+0.047}_{-0.024}$ (1.09)	$0.334^{+0.023}_{-0.040}$	$100.5^{+1.2}_{-1.0}$	–
DESI+DESY5	75^{+10}_{-8}	-0.084 ± 0.035 (2.38)	$0.375^{+0.026}_{-0.032}$	99.27 ± 0.81	–
DESI+PP	78^{+10}_{-9}	$-0.055^{+0.038}_{-0.025}$ (1.71)	$0.346^{+0.021}_{-0.030}$	100.09 ± 0.84	–
DESI+Union3	77^{+10}_{-10}	$-0.074^{+0.049}_{-0.034}$ (1.79)	$0.365^{+0.027}_{-0.043}$	$99.6^{+1.1}_{-0.98}$	–
PL18	63.1 ± 3.9	-0.0022 ± 0.0020 (1.09)	$0.383^{+0.051}_{-0.073}$	91.8 ± 6.9	0.867 ± 0.035
PL18+DESI	69.03 ± 0.42	0.00077 ± 0.00038 (2.01)	0.2947 ± 0.0047	101.63 ± 0.60	0.8202 ± 0.0099
PL18+DESI+DESY5	68.63 ± 0.40	0.00054 ± 0.00037 (1.45)	0.2993 ± 0.0046	101.06 ± 0.58	0.8213 ± 0.0099
PL18+DESI+PP	68.81 ± 0.40	0.00064 ± 0.00037 (1.76)	0.2972 ± 0.0046	101.32 ± 0.58	0.8209 ± 0.0098
PL18+DESI+Union3	68.85 ± 0.42	0.00067 ± 0.00037 (1.80)	0.2967 ± 0.0047	101.38 ± 0.59	0.8210 ± 0.0099
DESY3 (3×2pt)	82^{+20}_{-6}	$-0.0087^{+0.0067}_{-0.0058}$ (1.46)	$0.377^{+0.044}_{-0.066}$	$100.7^{+4.9}_{-7.1}$	0.766 ± 0.027
DESI+DESY3 (3×2pt)	> 80	$-0.0005^{+0.0035}_{-0.0026}$ (0.16)	$0.3007^{+0.0094}_{-0.011}$	101.32 ± 0.76	0.801 ± 0.017
DESI+DESY3 +DESY5	> 81.4	$-0.0025^{+0.0040}_{-0.0029}$ (0.73)	0.3148 ± 0.0094	100.35 ± 0.68	$0.794^{+0.017}_{-0.016}$

TABLE I. The mean $\pm 1\sigma$ constraints on the cosmological parameters inferred from the various datasets and their combinations considered in this letter for the ΛwDM scenario. In the bracket next to the w_{dm} we report the sigma deviation of w_{dm} from its expected value, zero. To calculate this, we compute the standard deviation $\sigma_{w_{\rm dm}}$ from the covariance matrix and tension is defined as the deviation of the mean ($\mu_{w_{\rm dm}}$) from zero in units of the standard deviation: $\frac{|\mu_{w_{\rm dm}}|}{\sigma_{w_{\rm dm}}}$. We note $\sim 2.4\,\sigma$ preference for $w_{\rm dm} < 0$ in DESI+DESY5 and discrepancy between DESI and Planck measurements.

a preference for non-vanishing $w_{\rm dm} = -0.084 \pm 0.035$ exceeding the 95% CL. Additionally, we find a higher value of $\Omega_{\rm m} = 0.375^{+0.026}_{-0.032}$ compared to ΛCDM and $H_0 = 75^{+10}_{-8}$. The large error bars on H_0 are due to the degeneracy between the Hubble parameter H_0 and the sound horizon at the drag epoch $z_{\rm d}$. The addition of CC data to DESI measurements breaks the $H_0\,r_{\rm d}$ degeneracy and does not affect the inference of a non-zero value of $w_{\rm dm}$ [90]. The 2-dimensional posterior distributions of $h\,r_{\rm d} - w_{\rm dm}$ and $\Omega_m - w_{\rm dm}$ for DESI and DESI+ SNIa are shown in Fig. 1 in the left and middle panels, respectively. It is clear from Fig. 1 that DESI and its combination with SNIa permit a wide range of posterior distribution of Ω_m. The ΛwDM scenario is statistically preferred over ΛCDM, with $\Delta\chi^2_{\rm MAP} \in [-3.4, -7.9]$ corresponding to significance levels ranging from 1.85σ to 2.80σ. We obtain a similar preference by evaluating the ΔDIC as shown in Table II. The combination of DESI + DESY5 shows a strong preference while DESI + PP and DESI + Union3 indicate moderate preferences over the concordance model.

Next, we investigate how CMB measurements affect the inference of dark matter EoS $w_{\rm dm}$. The PL18 measurements alone find the $w_{\rm dm} = -0.0022 \pm 0.0020$, $H_0 = 63.1 \pm 3.9$ and $\Omega_{\rm m} = 0.383^{+0.051}_{-0.073}$. We observe that the geometrical degeneracy compensates for extreme values of H_0 and Ω_m through the negative contribution of dark matter EoS. Both PL18 and DESI exclude $w_{\rm dm}$ from 0, but most of the posterior values of CMB inferred $w_{\rm dm}$ are not as widespread as those of DESI. The joint PL18+DESI analysis breaks the H_0-Ω_m-$w_{\rm dm}$ geometrical degeneracy, yielding $w_{\rm dm} = 0.00077 \pm 0.00038$ ($\sim 2\sigma$ from zero) and a higher H_0 than ΛCDM, though still in tension with $\rm SH_0ES$ [91, 92]. This combination shows moderate preference over ΛCDM, with $\Delta\chi^2_{\rm MAP} = -5.60$ and ΔDIC$= -3.32$. We also consider PL18 jointly with DESI and SNIa datasets, which even result in precise constraints on $w_{\rm dm}$. For instance, the most accurate constraint on $w_{\rm dm} = 0.00067 \pm 0.00037$ is derived from the PL18+DESI+Union3 combination. The $\Delta\chi^2_{\rm MAP}$ values are respectively $-3.82, -4.31$, and 4.03, indicating the

preference of the ΛwDM scenario over ΛCDM at $\approx 2\sigma$, for combining DESI with DESY5, PP and Union3, respectively. The similar preference can be corroborated from the last column of Table II using DIC except for the PP dataset. Hence, all combinations, including different SNIa measurements, consistently rule out $w_{\rm dm} = 0$ at least by 1.5σ.

Finally, we conclude our analysis by considering the DESY3 (3×2pt) in conjunction with DESI and SNIa data. First of all, unlike the SNIa measurements, $w_{\rm dm}$ can be inferred from DESY3 (3×2pt) alone, as shown in Table I. The right panel of Fig. 1 shows the comparison of one dimensional posterior distribution of $w_{\rm dm}$ obtained from DESI alone and in combination with DESY5 and DESY3 likelihood. We observe that weak lensing measurements, even when combined with DESI and supernova data, yield a dark matter EoS consistent with ΛCDM, although with significantly weaker constraints compared to other datasets. Consistent with previous analyses, we find substantial evidence favoring our model over ΛCDM, as demonstrated in Table II. Assessing the compatibility between different dataset combinations is essential, as joint analyses yield significantly different constraints. To quantify the concordance between two datasets (D_1 and D_2), we compute the DIC-based statistic $\mathcal{I}$. Table III presents the resulting $\log_{10}\mathcal{I}$ values for our dataset combinations. We find that combinations that favor $w_{\rm dm} < 0$ exhibit stronger concordance, while those predicting $w_{\rm dm} > 0$ show substantially lower compatibility.

The results obtained by combining DESI distance measurements with SNIa, CMB and DES-Y3 data clearly hint towards the preference of non-cold dark matter at varying level of significance. It is important to mention that such a preference is also present in DESI DR1. We have explicitly checked and found that our results are consistent with previous data release of DESI BAO. Furthermore, we also consider the SDSS BAO measurements from the final SDSS collaboration compilation comprising the eight effective redshift bins [10, 93]. Both DESI and SDSS datasets focus on the same distance measurements and have similar constraining power. Therefore, it is necessary to assess our results obtained from the DESI measurements. We perform MCMC analysis for SDSS by adopting the same methodology as used in the case of DESI. We find no evidence for non-vanishing EoS for dark matter component from the SDSS alone or from the joint analysis of SDSS with any SNIa compilations used in this work. In particular, we obtain a weak bound on $w_{\rm dm} < -0.0275$ using SDSS+DESY5. The analysis of other data such as Planck 2018 and DES-Y3 in conjunction with SDSS will not give much intuition in the inference of $w_{\rm dm} \neq 0$ as Planck and DES-Y3 alone can constrain $w_{\rm dm}$ precisely.

We further investigate how the constituent tracers of the DR2 samples at different redshifts affect our findings of $w_{\rm dm} < 0$. To do so, we split the DESI samples into two subsets based on the effective redshift, separating at $z = 1.1$. Interestingly, we see that the DESI DR 2 samples with $z > 1.1$ still provide $w_{\rm dm} < 0$ but consistent with $w_{\rm dm} = 0$ at varying CL for DESI and SNIa measurements, as shown in Table IV. The samples containing distances up to $z < 1.1$ are not able to constrain dark matter's EoS. Although, upon a close inspection it turns out that 90% of the posterior values of $w_{\rm dm}$ disfavor the possibility of cold dark matter.

Dataset	$\boldsymbol{\Delta\chi^2_{\rm MAP}}$	$\boldsymbol{N\sigma}$	**ΔDIC**
DESI	-0.5769	0.75	0.78
DESI+DESY5	-7.89	2.80	-5.87
DESI+PP	-3.43	1.85	-1.58
DESI+Union3	-4.08	2.02	-2.06
PL18	-0.10	0.32	-0.39
PL18+DESI	-5.60	2.36	-3.32
PL18+DESI+DESY5	-3.82	1.95	-2.32
PL18+DESI+PP	-4.31	2.07	-0.60
PL18+DESI+Union3	-4.03	2.0	-2.36
DESI+DESY3 (3×2pt)	-3.06	1.75	-4.65
DESI+DESY3(3×2pt)+DESY5	-2.69	1.64	-1.31

TABLE II. Comparison of ΛwDM versus ΛCDM using different statistical tests: the maximum a posteriori χ^2 difference ($\Delta\chi^2_{\rm MAP}$), significance level ($N\sigma$), and Deviance Information Criterion (ΔDIC). Negative $\Delta\chi^2_{\rm MAP}$ and ΔDIC values favor the ΛwDM, with DESI+DESY5 showing the strongest preference ($\Delta\chi^2_{\rm MAP} = -7.89$, 2.8σ significance) while combinations with Planck (PL18) yield weaker evidence.

Dataset (D_1&D_2)	$\log_{10}\ \mathcal{I}(\mathrm{D_1}, \mathrm{D_2})$
DESI & DESY5	0.94
DESI & PP	1.41
DESI & Union3	0.91
DESI & DESY3(3×2pt)	1.91
PL18 & DESI	0.84

TABLE III. DIC-based statistic $\log\mathcal{I}(D_1, D_2)$ quantifying tension between cosmological datasets. Positive values indicate agreement between datasets, with higher values corresponding to stronger consistency. Combinations favoring $w_{\rm dm} < 0$ show better concordance, while those predicting $w_{\rm dm} > 0$ yield significantly lower compatibility.

Dataset	$\boldsymbol{w_{\rm dm}}$	$\boldsymbol{\Omega_m}$	$\boldsymbol{h\,r_{\rm d}}$
DESI($z > 1.1$)	$-0.049^{+0.070}_{-0.022}$	$0.358^{+0.027}_{-0.089}$	$99.2^{+3.8}_{-2.7}$
DESI+DESY5	$-0.064^{+0.042}_{-0.033}$	$0.376^{+0.026}_{-0.031}$	97.8 ± 1.4
DESI+PP	$-0.043^{+0.039}_{-0.024}$	$0.347^{+0.023}_{-0.030}$	99.2 ± 1.5
DESI+Union3	$-0.068^{+0.055}_{-0.035}$	$0.380^{+0.033}_{-0.053}$	97.8 ± 1.8
DESI($z < 1.1$)	< -0.151	0.454 ± 0.090	99.1 ± 1.5
DESI+DESY5	< -0.220	$0.487^{+0.062}_{-0.055}$	98.8 ± 0.8
DESI+PP	$-0.184^{+0.065}_{-0.120}$	$0.425^{+0.052}_{-0.067}$	99.7 ± 0.8
DESI+Union3	< -0.217	$0.486^{+0.083}_{-0.056}$	98.6 ± 1.1

TABLE IV. 68% constraints on $w_{\rm dm}$, Ω_m, and $h\,r_{\rm d}$ from DESI BAO binned at $z > 1.1$ (consistent with ΛCDM) and $z < 1.1$ (favors $w_{\rm dm} < 0$), combined with DES-Y5, PP, and Union3 supernovae.

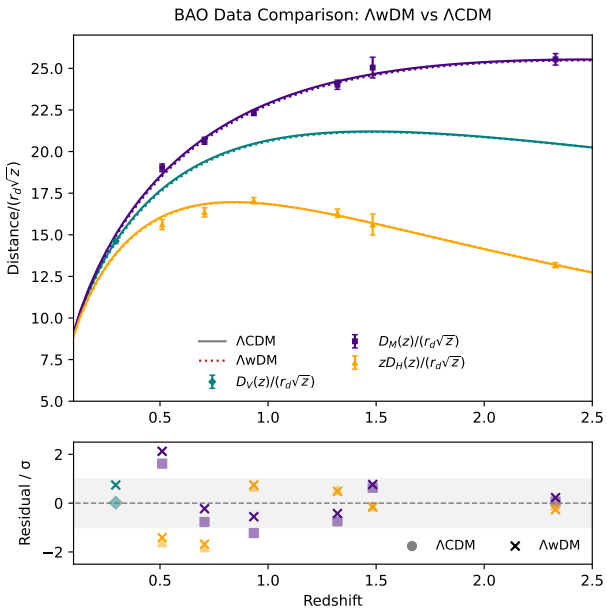

FIG. 2. *Upper Panel:* Comparison of rescaled distance-redshifts relations for ΛCDM (solid) and ΛwDM (dashed) model using the best-fit values inferred from DESI+Planck 2018 joint analysis. We also include the observational constraints with $\pm1\sigma$ uncertainty. Different type of distance measurements are indicated by different colors given in the legend. *Lower Panel:* The deviation of theoretical rescaled distances from the corresponding data-points in terms of σ. The predictions for ΛCDM and ΛwDM are shown by filled and cross shaped markers, respectively. The shaded region highlights the $\pm1\sigma$ range for reference.

To get a better understanding of the role played by DESI data, we also compare the theoretical distance predictions for ΛwDM and ΛCDM model with the observed distances probed by BAO measurements as shown in Fig. 2. The lower panel of Fig. 2 demonstrates that the theoretical distance deviations obtained using the ΛwDM model exhibit significant discrepancies with the concordance model for redshifts $z < 1.1$. In contrast, for $z > 1.1$, the results show strong agreement with the concordance model. Similar conclusions are also drawn from the analysis of the Binned DESI data discussed previously. Moreover, we observe that the primary contributor to the discrepancy between the models at $z < 1.1$ is the distance measure $D_{\rm M}(z)/(r_{\rm d}\sqrt{z})$.

Finally, we discuss the implications of the preference for $w_{\rm dm} < 0$ beyond the context explored in this work. As argued by the DESI collaboration, allowing for time-varying dark energy parametrized by the Chevallier-Polarski-Linder (CPL) form [94, 95] yields a strong statistical preference for such a scenario. A non-zero equation of state (EoS) for dark matter could naturally arise from interactions between the dark matter (DM) and dark energy (DE) sectors [96–98]. Indeed, multiple studies have reported evidence for a non-zero DM-DE coupling parameter [99**?** –105]. Alternatively, One can also envisage a scenario where DM and DE are described by a single fluid component [106–108]. Such Unified DM-DE (UDM) models have been shown to provide promising avenues for resolving both the Hubble tension and large-scale structure anomalies [109, 110].

In this letter, we have derived constraints on the dark matter equation of state parameter $w_{\rm dm}$ using the latest DESI BAO measurements, both independently and in combination with Planck, DES, and supernovae data. Our analysis reveals a robust preference for non-cold dark matter across multiple dataset combinations involving DESI. Notably, we observe a tension between background-based measurements (including SNIa compilations, cosmic chronometers, and BAO) and observations involving perturbations (such as Planck and DES Y3). The combination DESI+DESY5 yields $w_{\rm dm} = -0.084 \pm 0.035$, excluding the cold dark matter scenario ($w_{\rm dm} = 0$) at 2.4σ significance, while PL18+DESI gives $w_{\rm dm} = 0.00077 \pm 0.00038$, differing from the canonical value at 2σ. Although these estimates differ numerically, they both consistently suggest the existence of non-cold dark matter. We highlight that the preference for negative $w_{\rm dm}$ in DESI is primarily driven by low-redshift BAO measurements ($z < 1.1$), whereas higher redshift BAO data ($z > 1.1$) remain consistent with ΛCDM. Intriguingly, this evidence for $w_{\rm dm} < 0$ is more pronounced in DESI, as previous surveys like SDSS were only able to place weak constraints such a preference. For all dataset combinations considered, we observe significant improvements over the standard ΛCDM paradigm.

Our results demonstrate that the DESI dataset opens new avenues for investigating viable dark matter models via late-time physics. While this study focuses on the implications of DESI measurements for dark matter properties inferred from geometric distances, it is important to confirm these findings through full-shape modeling of the power spectrum, incorporating the effects of redshift-space distortions.

Note Added:- During the finalization of this work, [99, 102] appeared on arXiv, investigating dark matter properties with DESI data while incorporating interactions in the dark matter–dark energy (DM-DE) sector. In contrast, our analysis focuses on minimal extensions of the standard cosmological model and combines complete CMB power spectra measurements with DES-Y3 3×2 pt data. Unlike their findings, we observe a preference for the extended cosmological scenario over the ΛCDM.

Acknowledgments– We thank Prof. Ido Ben-Dayan and Prof. Sukanta Panda for their valuable comments. We also acknowledge the Open U HPC Center at Open University of Israel for providing computing resources that have contributed to the research results reported in this paper. We acknowledge Prof. Sunny Vagnozzi for providing the Python module utilized to create Fig. 2.

[1] N. Aghanim *et al.* (Planck), "Planck 2018 results. VI. Cosmological parameters," Astron. Astrophys. **641**, A6 (2020), [Erratum: Astron.Astrophys. 652, C4 (2021)], arXiv:1807.06209 [astro-ph.CO].

[2] N. Aghanim *et al.* (Planck), "Planck 2018 results. V. CMB power spectra and likelihoods," Astron. Astrophys. **641**, A5 (2020), arXiv:1907.12875 [astro-ph.CO].

[3] N. Aghanim *et al.* (Planck), "Planck 2018 results. VIII. Gravitational lensing," Astron. Astrophys. **641**, A8 (2020), arXiv:1807.06210 [astro-ph.CO].

[4] D. Dutcher *et al.* (SPT-3G), "Measurements of the E-mode polarization and temperature-E-mode correlation of the CMB from SPT-3G 2018 data," Phys. Rev. D **104**, 022003 (2021), arXiv:2101.01684 [astro-ph.CO].

[5] S. K. Choi *et al.* (ACT), "The Atacama Cosmology Telescope: a measurement of the Cosmic Microwave Background power spectra at 98 and 150 GHz," JCAP **12**, 045 (2020), arXiv:2007.07289 [astro-ph.CO].

[6] G. Hinshaw *et al.* (WMAP), "Nine-Year Wilkinson Microwave Anisotropy Probe (WMAP) Observations: Cosmological Parameter Results," Astrophys. J. Suppl. **208**, 19 (2013), arXiv:1212.5226 [astro-ph.CO].

[7] N. Aghanim *et al.* (Planck), "Planck 2018 results. I. Overview and the cosmological legacy of Planck," Astron. Astrophys. **641**, A1 (2020), arXiv:1807.06205 [astro-ph.CO].

[8] P. Lemos and P. Shah, "The Cosmic Microwave Background and H_0," (2023), arXiv:2307.13083 [astro-ph.CO].

[9] M. Tristram and K. Ganga, "Data analysis methods for the cosmic microwave background," Rept. Prog. Phys. **70**, 899 (2007), arXiv:0708.1429 [astro-ph].

[10] S. Alam *et al.* (BOSS), "The clustering of galaxies in the completed SDSS-III Baryon Oscillation Spectroscopic Survey: cosmological analysis of the DR12 galaxy sample," Mon. Not. Roy. Astron. Soc. **470**, 2617 (2017), arXiv:1607.03155 [astro-ph.CO].

[11] H. du Mas des Bourboux *et al.* (eBOSS), "The Completed SDSS-IV Extended Baryon Oscillation Spectroscopic Survey: Baryon Acoustic Oscillations with Lyα Forests," Astrophys. J. **901**, 153 (2020), arXiv:2007.08995 [astro-ph.CO].

[12] J. Hou *et al.* (eBOSS), "The Completed SDSS-IV extended Baryon Oscillation Spectroscopic Survey: BAO and RSD measurements from anisotropic clustering analysis of the Quasar Sample in configuration space between redshift 0.8 and 2.2," Mon. Not. Roy. Astron. Soc. **500**, 1201 (2020), arXiv:2007.08998 [astro-ph.CO].

[13] S. Alam *et al.* (eBOSS), "Completed SDSS-IV extended Baryon Oscillation Spectroscopic Survey: Cosmological implications from two decades of spectroscopic surveys at the Apache Point Observatory," Phys. Rev. D **103**, 083533 (2021), arXiv:2007.08991 [astro-ph.CO].

[14] H. Gil-Marin *et al.* (eBOSS), "The Completed SDSS-IV extended Baryon Oscillation Spectroscopic Survey: measurement of the BAO and growth rate of structure of the luminous red galaxy sample from the anisotropic power spectrum between redshifts 0.6 and 1.0," Mon. Not. Roy. Astron. Soc. **498**, 2492 (2020), arXiv:2007.08994 [astro-ph.CO].

[15] J. E. Bautista *et al.* (eBOSS), "The Completed SDSS-IV extended Baryon Oscillation Spectroscopic Survey: measurement of the BAO and growth rate of structure of the luminous red galaxy sample from the anisotropic correlation function between redshifts 0.6 and 1," Mon. Not. Roy. Astron. Soc. **500**, 736 (2020), arXiv:2007.08993 [astro-ph.CO].

[16] M. Abdul Karim *et al.* (DESI), "Data Release 1 of the Dark Energy Spectroscopic Instrument," (2025), arXiv:2503.14745 [astro-ph.CO].

[17] A. G. Adame *et al.* (DESI), "DESI 2024 VI: cosmological constraints from the measurements of baryon acoustic oscillations," JCAP **02**, 021 (2025), arXiv:2404.03002 [astro-ph.CO].

[18] D. M. Scolnic *et al.* (Pan-STARRS1), "The Complete Light-curve Sample of Spectroscopically Confirmed SNe Ia from Pan-STARRS1 and Cosmological Constraints from the Combined Pantheon Sample," Astrophys. J. **859**, 101 (2018), arXiv:1710.00845 [astro-ph.CO].

[19] D. Scolnic *et al.*, "The Pantheon+ Analysis: The Full Data Set and Light-curve Release," Astrophys. J. **938**, 113 (2022), arXiv:2112.03863 [astro-ph.CO].

[20] D. Rubin *et al.*, "Union Through UNITY: Cosmology with 2,000 SNe Using a Unified Bayesian Framework," (2023), arXiv:2311.12098 [astro-ph.CO].

[21] A. C. Bailey, M. Vincenzi, D. Scolnic, J. C. Cuillandre, J. Rhodes, I. Hook, E. R. Peterson, and B. Popovic, "Type Ia supernova observations combining data from the Euclid mission and the Vera C. Rubin Observatory," Mon. Not. Roy. Astron. Soc. **524**, 5432 (2023), arXiv:2211.01206 [astro-ph.CO].

[22] S. Blondin, "Type Ia supernovae," (2024), arXiv:2411.09740 [astro-ph.HE].

[23] T. M. C. Abbott *et al.* (DES), "The Dark Energy Survey: Cosmology Results with ~1500 New High-redshift Type Ia Supernovae Using the Full 5 yr Data Set," Astrophys. J. Lett. **973**, L14 (2024), arXiv:2401.02929 [astro-ph.CO].

[24] H. K. Fakhouri *et al.* (Nearby Supernova Factory), "Improving Cosmological Distance Measurements Using Twin Type Ia Supernovae," Astrophys. J. **815**, 58 (2015), arXiv:1511.01102 [astro-ph.CO].

[25] T. Abbott *et al.* (DES), "The Dark Energy Survey: more than dark energy – an overview," Mon. Not. Roy. Astron. Soc. **460**, 1270 (2016), arXiv:1601.00329 [astro-ph.CO].

[26] T. M. C. Abbott *et al.* (DES), "Cosmological Constraints from Multiple Probes in the Dark Energy Survey," Phys. Rev. Lett. **122**, 171301 (2019), arXiv:1811.02375 [astro-ph.CO].

[27] T. M. C. Abbott *et al.* (Linea Science Server, DES), "The Dark Energy Survey Data Release 2," Astrophys. J. Supp. **255**, 20 (2021), arXiv:2101.05765 [astro-ph.IM].

[28] H. Hildebrandt *et al.*, "KiDS-450: Cosmological parameter constraints from tomographic weak gravitational lensing," Mon. Not. Roy. Astron. Soc. **465**, 1454 (2017), arXiv:1606.05338 [astro-ph.CO].

[29] H. Hildebrandt *et al.*, "KiDS+VIKING-450: Cosmic shear tomography with optical and infrared data," Astron. Astrophys. **633**, A69 (2020), arXiv:1812.06076 [astro-ph.CO].
[30] C. Hikage *et al.* (HSC), "Cosmology from cosmic shear power spectra with Subaru Hyper Suprime-Cam first-year data," Publ. Astron. Soc. Jap. **71**, 43 (2019), arXiv:1809.09148 [astro-ph.CO].
[31] T. M. C. Abbott *et al.* (DES), "Dark Energy Survey Year 3 results: Constraints on extensions to ΛCDM with weak lensing and galaxy clustering," Phys. Rev. D **107**, 083504 (2023), arXiv:2207.05766 [astro-ph.CO].
[32] T. M. C. Abbott *et al.* (DES), "Dark Energy Survey Year 3 results: Cosmological constraints from galaxy clustering and weak lensing," Phys. Rev. D **105**, 023520 (2022), arXiv:2105.13549 [astro-ph.CO].
[33] C. J. Copi, D. Huterer, D. J. Schwarz, and G. D. Starkman, "Lack of large-angle TT correlations persists in WMAP and Planck," Mon. Not. Roy. Astron. Soc. **451**, 2978 (2015), arXiv:1310.3831 [astro-ph.CO].
[34] C. Copi, D. Huterer, D. Schwarz, and G. Starkman, "The Uncorrelated Universe: Statistical Anisotropy and the Vanishing Angular Correlation Function in WMAP Years 1-3," Phys. Rev. D **75**, 023507 (2007), arXiv:astro-ph/0605135.
[35] J. S. Bullock and M. Boylan-Kolchin, "Small-Scale Challenges to the CDM Paradigm," Ann. Rev. Astron. Astrophys. **55**, 343 (2017), arXiv:1707.04256 [astro-ph.CO].
[36] H. J. de Vega, P. Salucci, and N. G. Sanchez, "Observational rotation curves and density profiles versus the Thomas Fermi galaxy structure theory," Mon. Not. Roy. Astron. Soc. **442**, 2717 (2014), arXiv:1309.2290 [astro-ph.CO].
[37] A. A. Klypin, A. V. Kravtsov, O. Valenzuela, and F. Prada, "Where are the missing Galactic satellites?" Astrophys. J. **522**, 82 (1999), arXiv:astro-ph/9901240.
[38] B. Moore, S. Ghigna, F. Governato, G. Lake, T. R. Quinn, J. Stadel, and P. Tozzi, "Dark matter substructure within galactic halos," Astrophys. J. Lett. **524**, L19 (1999), arXiv:astro-ph/9907411.
[39] M. Boylan-Kolchin, J. S. Bullock, and M. Kaplinghat, "Too big to fail? The puzzling darkness of massive Milky Way subhaloes," mnras **415**, L40 (2011), arXiv:1103.0007 [astro-ph.CO].
[40] S. Dodelson and L. M. Widrow, "Sterile-neutrinos as dark matter," Phys. Rev. Lett. **72**, 17 (1994), arXiv:hep-ph/9303287.
[41] M. R. Lovell, S. Bose, A. Boyarsky, S. Cole, C. S. Frenk, V. Gonzalez-Perez, R. Kennedy, O. Ruchayskiy, and A. Smith, "Satellite galaxies in semi-analytic models of galaxy formation with sterile neutrino dark matter," Mon. Not. Roy. Astron. Soc. **461**, 60 (2016), arXiv:1511.04078 [astro-ph.CO].
[42] M. Cortês and A. R. Liddle, "Interpreting DESI's evidence for evolving dark energy," JCAP **12**, 007 (2024), arXiv:2404.08056 [astro-ph.CO].
[43] B. Ratra and P. J. E. Peebles, "Cosmological consequences of a rolling homogeneous scalar field," Phys. Rev. D **37**, 3406 (1988).
[44] T. Chiba, N. Sugiyama, and T. Nakamura, "Cosmology with x matter," Mon. Not. Roy. Astron. Soc. **289**, L5 (1997), arXiv:astro-ph/9704199.
[45] T. Chiba, T. Okabe, and M. Yamaguchi, "Kinetically driven quintessence," Phys. Rev. D **62**, 023511 (2000).
[46] C. Armendariz-Picon, V. Mukhanov, and P. J. Steinhardt, "Essentials of k-essence," Phys. Rev. D **63**, 103510 (2001).
[47] T. P. Sotiriou and V. Faraoni, "f(R) Theories Of Gravity," Rev. Mod. Phys. **82**, 451 (2010), arXiv:0805.1726 [gr-qc].
[48] M. T. Manoharan, N. Shaji, and T. K. Mathew, "Holographic dark energy from the laws of thermodynamics with Rényi entropy," Eur. Phys. J. C **83**, 19 (2023), arXiv:2208.08736 [gr-qc].
[49] M. Rinaldi, "Higgs Dark Energy," Class. Quant. Grav. **32**, 045002 (2015), arXiv:1404.0532 [astro-ph.CO].
[50] W. Hu and I. Sawicki, "Models of f(R) Cosmic Acceleration that Evade Solar-System Tests," Phys. Rev. D **76**, 064004 (2007), arXiv:0705.1158 [astro-ph].
[51] A. Casalino, M. Rinaldi, L. Sebastiani, and S. Vagnozzi, "Mimicking dark matter and dark energy in a mimetic model compatible with GW170817," Phys. Dark Univ. **22**, 108 (2018), arXiv:1803.02620 [gr-qc].
[52] U. Mukhopadhyay and D. Majumdar, "Swampland criteria in the slotheon field dark energy," Phys. Rev. D **100**, 024006 (2019), arXiv:1904.01455 [gr-qc].
[53] Ruchika, S. A. Adil, K. Dutta, A. Mukherjee, and A. A. Sen, "Observational constraints on axion(s) dark energy with a cosmological constant," Phys. Dark Univ. **40**, 101199 (2023), arXiv:2005.08813 [astro-ph.CO].
[54] S. D. Odintsov, V. K. Oikonomou, and T. Paul, "From a Bounce to the Dark Energy Era with $F(R)$ Gravity," Class. Quant. Grav. **37**, 235005 (2020), arXiv:2009.09947 [gr-qc].
[55] Y. C. Ong, "An Effective Sign Switching Dark Energy: Lotka–Volterra Model of Two Interacting Fluids," Universe **9**, 437 (2023), arXiv:2212.04429 [gr-qc].
[56] G. G. Luciano, "Saez–Ballester gravity in Kantowski–Sachs Universe: A new reconstruction paradigm for Barrow Holographic Dark Energy," Phys. Dark Univ. **41**, 101237 (2023), arXiv:2301.12488 [gr-qc].
[57] U. K. Tyagi, S. Haridasu, and S. Basak, "Constraints on Generalized Gravity-Thermodynamic Cosmology from DESI DR2," (2025), arXiv:2504.11308 [astro-ph.CO].
[58] Y. Akrami, G. Alestas, and S. Nesseris, "Has DESI detected exponential quintessence?" (2025), arXiv:2504.04226 [astro-ph.CO].
[59] F. B. M. d. Santos, J. Morais, S. Pan, W. Yang, and E. Di Valentino, "A New Window on Dynamical Dark Energy: Combining DESI-DR2 BAO with future Gravitational Wave Observations," (2025), arXiv:2504.04646 [astro-ph.CO].
[60] E. O. Colgáin, S. Pourojaghi, M. M. Sheikh-Jabbari, and L. Yin, "How much has DESI dark energy evolved since DR1?" (2025), arXiv:2504.04417 [astro-ph.CO].
[61] M. Artymowski, I. Ben-Dayan, and U. Kumar, "Emergent dark energy from unparticles," Phys. Rev. D **103**, L121303 (2021), arXiv:2010.02998 [hep-ph].
[62] I. Ben-Dayan and U. Kumar, "Emergent Unparticles Dark Energy can restore cosmological concordance," JCAP **12**, 047 (2023), arXiv:2302.00067 [astro-ph.CO].

[63] I. Ben-Dayan and U. Kumar, "Theoretical priors and the dark energy equation of state," Eur. Phys. J. C **84**, 167 (2024), arXiv:2310.03092 [astro-ph.CO].
[64] L. Amendola, "Coupled quintessence," Phys. Rev. D **62**, 043511 (2000), arXiv:astro-ph/9908023.
[65] R. An, C. Feng, and B. Wang, "Relieving the Tension between Weak Lensing and Cosmic Microwave Background with Interacting Dark Matter and Dark Energy Models," JCAP **02**, 038 (2018), arXiv:1711.06799 [astro-ph.CO].
[66] W. Yang, N. Banerjee, and S. Pan, "Constraining a dark matter and dark energy interaction scenario with a dynamical equation of state," Phys. Rev. D **95**, 123527 (2017), [Addendum: Phys.Rev.D 96, 089903 (2017)], arXiv:1705.09278 [astro-ph.CO].
[67] E. Di Valentino, A. Melchiorri, O. Mena, and S. Vagnozzi, "Interacting dark energy in the early 2020s: A promising solution to the H_0 and cosmic shear tensions," Phys. Dark Univ. **30**, 100666 (2020), arXiv:1908.04281 [astro-ph.CO].
[68] T. Patil, Ruchika, and S. Panda, "Coupled quintessence scalar field model in light of observational datasets," JCAP **05**, 033 (2024), arXiv:2307.03740 [astro-ph.CO].
[69] M. A. van der Westhuizen and A. Abebe, "Interacting dark energy: clarifying the cosmological implications and viability conditions," JCAP **01**, 048 (2024), arXiv:2302.11949 [gr-qc].
[70] Ashmita, K. Banerjee, and P. K. Das, "Constructing viable interacting dark matter and dark energy models: a dynamical systems approach," JCAP **11**, 034 (2024), arXiv:2410.02261 [gr-qc].
[71] J. M. Gomes, E. Hardy, and S. Parameswaran, "Dark energy with the help of interacting dark sectors," Phys. Rev. D **110**, 023533 (2024), arXiv:2311.08888 [hep-ph].
[72] S. Kumar and L. Xu, "Observational constraints on variable equation of state parameters of dark matter and dark energy after Planck," Phys. Lett. B **737**, 244 (2014), arXiv:1207.5582 [gr-qc].
[73] C. M. Muller, "Cosmological bounds on the equation of state of dark matter," Phys. Rev. D **71**, 047302 (2005), arXiv:astro-ph/0410621.
[74] C. Armendariz-Picon and J. T. Neelakanta, "How Cold is Cold Dark Matter?" JCAP **03**, 049 (2014), arXiv:1309.6971 [astro-ph.CO].
[75] M. Kopp, C. Skordis, D. B. Thomas, and S. Ilić, "Dark Matter Equation of State through Cosmic History," Phys. Rev. Lett. **120**, 221102 (2018), arXiv:1802.09541 [astro-ph.CO].
[76] C.-P. Ma and E. Bertschinger, "Cosmological perturbation theory in the synchronous and conformal Newtonian gauges," Astrophys. J. **455**, 7 (1995), arXiv:astro-ph/9506072.
[77] L. Xu and Y. Chang, "Equation of State of Dark Matter after Planck Data," Phys. Rev. D **88**, 127301 (2013), arXiv:1310.1532 [astro-ph.CO].
[78] A. Lewis, A. Challinor, and A. Lasenby, "Efficient computation of CMB anisotropies in closed FRW models," Astrophys. J. **538**, 473 (2000), arXiv:astro-ph/9911177.
[79] C. Howlett, A. Lewis, A. Hall, and A. Challinor, "CMB power spectrum parameter degeneracies in the era of precision cosmology," jcap **2012**, 027 (2012), arXiv:1201.3654 [astro-ph.CO].
[80] J. Torrado and A. Lewis, "Cobaya: Code for Bayesian Analysis of hierarchical physical models," JCAP **05**, 057 (2021), arXiv:2005.05290 [astro-ph.IM].
[81] J. Torrado and A. Lewis, "Cobaya: Bayesian analysis in cosmology," Astrophysics Source Code Library, record ascl:1910.019 (2019).
[82] A. Lewis, "GetDist: a Python package for analysing Monte Carlo samples," (2019), arXiv:1910.13970 [astro-ph.IM].
[83] C. Cartis, J. Fiala, B. Marteau, and L. Roberts, "Improving the Flexibility and Robustness of Model-Based Derivative-Free Optimization Solvers," arXiv e-prints , arXiv:1804.00154 (2018), arXiv:1804.00154 [math.OC].
[84] C. Cartis, L. Roberts, and O. Sheridan-Methven, "Escaping local minima with derivative-free methods: a numerical investigation," arXiv e-prints , arXiv:1812.11343 (2018), arXiv:1812.11343 [math.OC].
[85] S. Vagnozzi, E. Di Valentino, S. Gariazzo, A. Melchiorri, O. Mena, and J. Silk, "The galaxy power spectrum take on spatial curvature and cosmic concordance," Phys. Dark Univ. **33**, 100851 (2021), arXiv:2010.02230 [astro-ph.CO].
[86] S. Joudaki *et al.*, "CFHTLenS revisited: assessing concordance with Planck including astrophysical systematics," Mon. Not. Roy. Astron. Soc. **465**, 2033 (2017), arXiv:1601.05786 [astro-ph.CO].
[87] M. Abdul Karim *et al.* (DESI), "DESI DR2 Results II: Measurements of Baryon Acoustic Oscillations and Cosmological Constraints," (2025), arXiv:2503.14738 [astro-ph.CO].
[88] M. Abdul Karim *et al.* (DESI), "DESI DR2 Results I: Baryon Acoustic Oscillations from the Lyman Alpha Forest," (2025), arXiv:2503.14739 [astro-ph.CO].
[89] E. Krause and T. Eifler, "cosmolike – cosmological likelihood analyses for photometric galaxy surveys," Mon. Not. Roy. Astron. Soc. **470**, 2100 (2017), arXiv:1601.05779 [astro-ph.CO].
[90] The cosmic chronometers (CC) method relates the evolution of differential ages of passive galaxies at different redshifts without assuming any cosmological model [**?**]. We use the 32 measurements of Hubble parameter along with their covariance matrix.
[91] A. G. Riess *et al.*, "A 2.4% Determination of the Local Value of the Hubble Constant," Astrophys. J. **826**, 56 (2016), arXiv:1604.01424 [astro-ph.CO].
[92] A. G. Riess, S. Casertano, W. Yuan, J. B. Bowers, L. Macri, J. C. Zinn, and D. Scolnic, "Cosmic Distances Calibrated to 1% Precision with Gaia EDR3 Parallaxes and Hubble Space Telescope Photometry of 75 Milky Way Cepheids Confirm Tension with ΛCDM," Astrophys. J. Lett. **908**, L6 (2021), arXiv:2012.08534 [astro-ph.CO].
[93] A. J. Ross *et al.* (BOSS), "The clustering of galaxies in the completed SDSS-III Baryon Oscillation Spectroscopic Survey: Observational systematics and baryon acoustic oscillations in the correlation function," Mon. Not. Roy. Astron. Soc. **464**, 1168 (2017), arXiv:1607.03145 [astro-ph.CO].

[94] M. Chevallier and D. Polarski, "Accelerating universes with scaling dark matter," Int. J. Mod. Phys. D **10**, 213 (2001), arXiv:gr-qc/0009008.

[95] E. V. Linder, "Exploring the expansion history of the universe," Phys. Rev. Lett. **90**, 091301 (2003), arXiv:astro-ph/0208512.

[96] J.-H. He and B. Wang, "Effects of the interaction between dark energy and dark matter on cosmological parameters," JCAP **06**, 010 (2008), arXiv:0801.4233 [astro-ph].

[97] M. B. Gavela, D. Hernandez, L. Lopez Honorez, O. Mena, and S. Rigolin, "Dark coupling," JCAP **07**, 034 (2009), [Erratum: JCAP 05, E01 (2010)], arXiv:0901.1611 [astro-ph.CO].

[98] T. Clemson, K. Koyama, G.-B. Zhao, R. Maartens, and J. Valiviita, "Interacting Dark Energy – constraints and degeneracies," Phys. Rev. D **85**, 043007 (2012), arXiv:1109.6234 [astro-ph.CO].

[99] W. Yang, S. Pan, E. Di Valentino, O. Mena, D. F. Mota, and S. Chakraborty, "Probing the cold nature of dark matter," (2025), arXiv:2504.11973 [astro-ph.CO].

[100] S. Pan, W. Yang, E. Di Valentino, D. F. Mota, and J. Silk, "IWDM: the fate of an interacting non-cold dark matter — vacuum scenario," JCAP **07**, 064 (2023), arXiv:2211.11047 [astro-ph.CO].

[101] W.-T. Hou, J.-Z. Qi, T. Han, J.-F. Zhang, S. Cao, and X. Zhang, "Prospects for constraining interacting dark energy models from gravitational wave and gamma ray burst joint observation," JCAP **05**, 017 (2023), arXiv:2211.10087 [astro-ph.CO].

[102] S. Pan, S. Paul, E. N. Saridakis, and W. Yang, "Interacting dark energy after DESI DR2: a challenge for ΛCDM paradigm?" (2025), arXiv:2504.00994 [astro-ph.CO].

[103] W. Giarè, M. A. Sabogal, R. C. Nunes, and E. Di Valentino, "Interacting Dark Energy after DESI Baryon Acoustic Oscillation Measurements," Phys. Rev. Lett. **133**, 251003 (2024), arXiv:2404.15232 [astro-ph.CO].

[104] E. Silva, M. A. Sabogal, M. S. Souza, R. C. Nunes, E. Di Valentino, and S. Kumar, "New Constraints on Interacting Dark Energy from DESI DR2 BAO Observations," (2025), arXiv:2503.23225 [astro-ph.CO].

[105] D. A. Kessler, L. A. Escamilla, S. Pan, and E. Di Valentino, "One-parameter dynamical dark energy: Hints for oscillations," (2025), arXiv:2504.00776 [astro-ph.CO].

[106] F. K. Anagnostopoulos, D. Benisty, S. Basilakos, and E. I. Guendelman, "Dark energy and dark matter unification from dynamical space time: observational constraints and cosmological implications," JCAP **06**, 003 (2019), arXiv:1904.05762 [gr-qc].

[107] D. Perkovic and H. Stefancic, "Dark sector unifications: dark matter-phantom energy, dark matter - constant w dark energy, dark matter-dark energy-dark matter," Phys. Lett. B **797**, 134806 (2019), arXiv:1902.05365 [gr-qc].

[108] G. Koutsoumbas, K. Ntrekis, E. Papantonopoulos, and E. N. Saridakis, "Unification of Dark Matter - Dark Energy in Generalized Galileon Theories," JCAP **02**, 003 (2018), arXiv:1704.08640 [gr-qc].

[109] E. Frion, D. Camarena, L. Giani, T. Miranda, D. Bertacca, V. Marra, and O. F. Piattella, "Bayesian analysis of a Unified Dark Matter model with transition: can it alleviate the H_0 tension?" (2023), 10.21105/astro.2307.06320, arXiv:2307.06320 [astro-ph.CO].

[110] M. Hashim and A. A. El-Zant, "Clustered unified dark sector cosmology: Background evolution and linear perturbations in light of observations," Phys. Rev. D **111**, 063522 (2025).

COMPARISON OF DESI AND SDSS COSNTRAINTS

In this extended analysis, we build upon the study presented in the main text by substituting the DESI dataset with the Baryon Acoustic Oscillation (BAO) measurements obtained from the final compilation of the SDSS collaboration. This dataset encompasses a comprehensive set of observations across eight distinct redshift intervals, providing an alternative yet consistent framework for examining the same cosmological parameters. The specific redshift ranges and corresponding measurements are detailed in [13]. As in the previous analysis, we incorporate the BAO dataset in combination with additional cosmological probes, including the DESY5 galaxy clustering data, PantheonPlus (PP) measurements, and the Union 3 compilation of Type Ia supernova observations, to ensure a comprehensive and robust constraint on the model parameters.

We summarize the observational constraints derived from our analysis in Table V. Notably, we do not obtain any robust constraints on the dark matter equation-of-state parameter, w_{dm}, regardless of the combination of datasets considered. However, our results consistently indicate a higher value of the matter density parameter, Ω_m, and a lower value of the product $h\,r_d$, compared to our analysis with the DESI.

Dataset	$\boldsymbol{H_0}$	$\boldsymbol{w_{dm}}$	$\boldsymbol{\Omega_m}$	$\boldsymbol{h\,r_{\rm d}}$
SDSS	75^{+20}_{-10}	< -0.0256	$0.413^{+0.058}_{-0.076}$	97.5 ± 2.2
SDSS+DESY5	76^{+20}_{-10}	< -0.0321	$0.384^{+0.026}_{-0.030}$	$98.5^{1.00}_{0.92}$
SDSS+PP	77^{+20}_{-9}	< -0.0290	$0.363^{+0.026}_{-0.032}$	99.2 ± 1.0
SDSS+Union3	74^{+20}_{-10}	< -0.0201	$0.390^{+0.032}_{-0.040}$	$98.1^{1.10}_{0.96}$

TABLE V. 68% constraints on $w_{\rm dm}$, Ω_m, and $h\,r_{\rm d}$ from SDSS BAO alone and combined with DES-Y5, PP, and Union3 supernovae.